




Design Method of Electrical Automation Control System Infrastructure based on Path Optimization Hybrid Algorithm

Pengxiao Ji¹*

¹School of Electrical Engineering, Zhengzhou Railway Vocational & Technical College, Zhengzhou, Henan 451460, China

Corresponding author: Pengxiao Ji, jipengxiao@zzrvtc.edu.cn

Abstract. In order to improve the control effect of the electrical automation control system (EACS), this paper combines the path optimization algorithm to design the EACS, and takes the control of the AGV vehicle as a case to study the algorithm effect. Moreover, this paper uses ACA and multi-agent system as the theoretical basis for AGV path optimization. In addition, this paper improves the ACA from the pheromone feedback mechanism, pheromone update rules and state rules, and integrates it into the multi-agent system, innovatively introduces the concept of crowding degree, and sets the threshold of crowding degree. Aiming at the path conflict existing in AGV, this paper constructs a conflict detection model and designs a conflict resolution mechanism.

Keywords: path optimization hybrid algorithm; electrical; automation; control system, Advancing Infrastructure Development

DOI: <https://doi.org/10.14733/cadaps.2023.S15.114-129>

1 INTRODUCTION

Push the pneumatic film of the driving device through the air pressure to control the fluid in the pipeline. The regulating valve is the part of the electrical control center connected with the pipeline, which can realize the regulation of flow, pressure and temperature [1]. The valve positioner is used to ensure that the automatic control system (ACS) is in the position specified by the controller. The positioner is based on the pressure change to adjust the position change to ensure the balance between the control signal and the valve stem position. When carrying out the power and electrical energy-saving system, the designer needs to select the type of valve based on the full grasp. In this process, the designer must consider both the economic cost and the performance of the valve [2].

At present, the voltage energy-saving control of the power and EACS has realized the accurate judgment of some specific scenarios, and can rely on intelligent means to control the opening and

closing of the circuit. Some progress has been made in voltage energy saving, but it still cannot meet the increasing energy saving of users. The high-quality, high-efficiency and energy-saving control of the voltage of the power and EACS has not yet been realized [3]. This is mainly because the composition of the power and EACS is complex, which leads to various disturbances during the voltage transmission and control inside it, which causes the control signal to have large errors under the influence of voltage fluctuations, resulting in the expression of electrical control and regulation system in voltage control is not accurate, and it is difficult to ensure the transmission and supply of voltage with high quality and efficiency. In particular, the long-term working state of power and electrical equipment is affected by voltage fluctuations, which not only easily causes large energy consumption, but also seriously affects the service life of the equipment. Based on this, an advanced control method must be proposed to optimize it [4]. At present, many technicians have taken the electrical control and regulation system as the voltage work unit, and on this basis, control the voltage of the power and electrical equipment. In the process of exploring new methods, the researchers strengthened the experiments on the voltage regulation method based on the multi-layer neural network. By designing the voltage signal denoising model to eliminate the ambiguity and fluctuation in the voltage control, the error of the control signal was effectively solved. To further improve the level of intelligent voltage management and control, so as to achieve a higher level of power saving [5].

The voltage of the ACS should be kept constant and the error caused by the control consumption should be eliminated. However, the reality is that the voltage of the power and EACS often fluctuates, and the control signals of each key part have large errors, which have a great impact on the control accuracy and are prone to increasing energy consumption. In order to make the voltage energy saving of the ACS ideal, we need to adhere to the principle of "simplification of complex problems", and use the method of setting parameters to solve the error problem. By introducing a parameter into the whole system and mathematically processing this parameter, the error caused by voltage fluctuation can be accurately grasped, and the purpose of high-quality and high-efficiency control of energy consumption can be achieved [6]. The value change of the selected parameter needs to directly reflect the voltage change and its influence on the system control. For example, when the voltage fluctuation is abnormal, a mathematical model is constructed by using the relationship between the voltage and its fluctuation rate and fluctuation amplitude coefficient [7]. When the voltage fluctuation is large, the above method is still used to count the error generated by the voltage signal, and then the influence of the voltage fluctuation on the system control effect is detected according to the voltage fluctuation law. Involving multiple sets of data, it is necessary to collect and record these data, and conduct comprehensive and partial analysis. In particular, the change of each variability control coefficient should be normalized in the interval of $(-1, 1)$ to limit the fluctuation range of the voltage [8]. Then according to the hypothetical method, standardize these irregular changes, and then adopt the optimal correlation control method to adjust these parameters, so as to realize the powerful control of the fluctuation interference existing in the EACS, so as to achieve better Energy saving effect [9]. Infrastructure development plays a crucial role in achieving the desired energy-saving effect of the ACS.

When studying the effect of quantization, it is necessary to set a quantization function to reasonably represent the actual voltage parameters of the electric power ACS, and then rely on the method of solving the function equation to seek the optimal solution, so as to realize the scientific setting of the relevant parameters. When voltage fluctuations occur, by measuring each control signal in time and accurately, and relying on the quantitative function relationship to analyze multiple sets of parameters, we can clearly understand the relationship between signal-to-noise and response time [10]. In order to achieve effective energy-saving control during the control period, it is also necessary to find the optimal combination of the variation of the voltage fluctuation rate parameter, and adjust

it according to the requirements of the optimal specification when eliminating interference to obtain the optimal energy-saving combination value. At the same time, in order to reduce the impact of voltage fluctuations on the power system, it is also necessary to formulate a reasonable setting standard to solve the interference caused by voltage fluctuations [11]. In particular, the setting of such parameters is specified strictly according to the specification requirements, and the optimal combination of these parameters is carried out to solve the problem of minimum gate voltage fluctuation interference in the ACS, so as to find a more reasonable control method. In general, for the voltage energy-saving control of the power and EACS, it is to build a function model, rely on mathematical ideas to solve the equation, and carry out the optimal combination of the involved parameters, so as to ensure the minimum energy consumption of the power system and achieve effective energy saving. [12].

The overall performance of power consumption determines the energy-saving performance of the power and EACS. At the same time, the voltage of the electrical control and regulation system is closely related to the energy-saving performance of the system. In order to effectively achieve the purpose of energy saving [13]. As an advanced control method, the control method based on the multi-layer neural network is more in line with the requirements of the voltage energy-saving control of the electric power ACS, and can implement precise control of the voltage of the ACS by relying on intelligent energy-saving adjustment. In particular, its neural network is a kind of feedforward network, nonlinearity is the main feature of voltage change in the ACS, and linearity is the main feature of the input layer and output layer of the neural network [14]. By taking the input layer data as the voltage control parameter of the ACS and the output layer data as the optimal voltage parameter, the multi-layer neural network processing of the dynamic change of the voltage in the power and EACS can be realized, which can effectively improve the voltage energy-saving control [15].

By analyzing the actual parameter response curves of the power and EACS before and after the energy-saving control, it can be seen that this model can intuitively show the change characteristics of the energy-saving characteristics before and after the voltage optimization in the power and EACS, and can reflect the model in power operation. Whether the actual voltage fluctuation is effectively controlled during the period [16]. If the error is controlled within a small and reasonable range, it means that the method can effectively control the voltage fluctuation in the electric power ACS; if the error cannot be controlled within a small range, it means that the method cannot improve the The energy-saving control effect of the power and EACS needs to redesign the model and adjust the parameters [17]. When analyzing the experimental results, it should be noted that the fluctuation range of the input current of the simulated power equipment changes with the change of the parameters. If the fluctuation range of the voltage control time is small at this time, or exceeds the range limit, the fluctuation range of the voltage control parameters will also If there is no obvious change, it shows that the effect of controlling the voltage in the electric power ACS based on the model is ideal, and it is proved that limiting the control error to a small range can realize the control of the voltage fluctuation of the electric control regulation system in the power operation. Good regulation and control, will not consume too much power [18].

This paper combines the path optimization algorithm to implement the design of the EACS, and proposes an EACS to effectively improve the control effect of the system.

2 ELECTRICAL AUTOMATION CONTROL ALGORITHM BASED ON PATH OPTIMIZATION HYBRID ALGORITHM

This paper combines the path optimization hybrid algorithm to study the algorithm effect by taking the control of AGV vehicles as a case.

2.1 Improvement of Ant Colony Algorithm (ACA)

Since different types of systems control AGV in different ways, the following assumptions are made for the system of algorithm and model research:

- 1.The system is a centralized structure MAS, and all instructions are sent to each AGV by the central control system (CCS).
- 2.There is no information communication between AGVs in the system.
- 3.The transportation road network of the system consists of road segments and nodes.
- 4.Two or more AGVs are not allowed to drive side by side on each road section.
- 5.Each node does not allow two or more AGVs to pass through at the same time.
- 6.The influence of external uncontrollable factors such as environment and weather on the system is not considered.

Among them, assumption (1) sets the external structure of the system. Assumption (2) sets the information communication of AGV in the system. Assumption (3) sets the composition of the transportation network in the system. Assumption (4)(5) sets the driving mode of the AGV. Assumption (6) sets the factors that affect the system. The structure of the AGV transportation system is shown in Figure 1. Each AGV in the system uploads location and driving information to the CCS in real time, and the CCS generates driving instructions based on the information and sends them to each AGV.

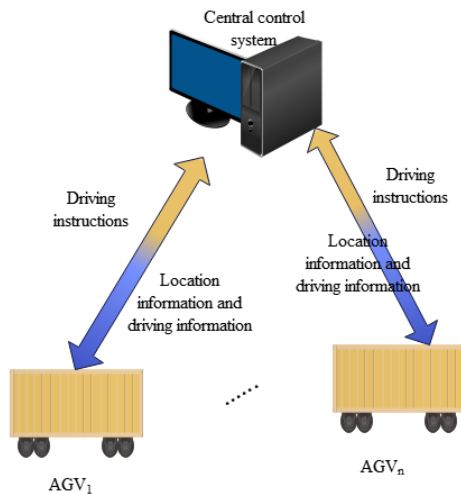


Figure 1: Schematic diagram of the automated terminal AGV transportation system.

2.2 Ant Agent and Congestion

The ACA imitates ants foraging, allowing ants to search for paths by releasing pheromones. The AGV is regarded as an Ant-agent, so that the AGV has the characteristics of both ants and agents, and the ACA is integrated into the MAS.

The AGV transportation system needs to control multiple AGVs to drive on the transportation network at the same time. If it is the same as the traditional ant colony algorithm, the pheromone is a positive feedback mechanism, and the AGV will generate path conflicts and collisions. At the same time, due to the long distance between the intersections of each road segment, the pheromone

concentrations that can be perceived at different locations on the same road segment at the same time are different. If the road section is used as a pheromone carrier, the degree of rejection of each AGV by this road section cannot be accurately represented. Therefore, the following restrictions are proposed for Ant-agent (AGV).

The pheromone is sensed at the intersection of the path, and the sum of the pheromone concentration is the crowding degree of the point.

The above limitations limit the pheromone properties of Ant-agent. The pheromone can reflect the characteristics of the environmental state and use the sum of the pheromone concentrations sensed by each node to express the degree of crowding here.

In order to realize the real-time control of AGV, a real-time global update strategy of congestion degree is adopted, and the congestion degree of each node is updated according to the positions of all AGVs in the transportation network at each moment.

$$\eta_{ij} = \frac{1}{d_{ij}}$$

The traditional ACA uses the heuristic function $\eta_{ij} = \frac{1}{d_{ij}}$ to represent the visibility between two points. Using the principle of visibility, the pheromone concentration perceived by the node decreases with the increase of the distance from the AGV, as shown in Figure 2.

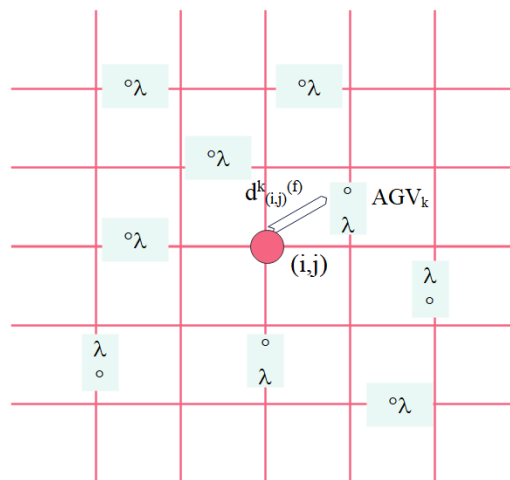


Figure 2: Schematic diagram of pheromone perception.

Taking any node (i, j) as an example, at time t , the pheromone concentration of the perceived AG

V_k (the k th AGV) is $\lambda \cdot \frac{1}{d_{(i,j)}^k(t)}$. Therefore, at time t , the congestion degree $\tau_{(i,j)}(t)$ at any node (i, j) in the transportation network is:

$$\tau_{(i,j)}(t) = \begin{cases} \sum_{k=1}^n \left(\lambda \cdot \frac{1}{d_{(i,j)}^k(t)} \right), & \text{AGVs are in operation} \\ 0, & \text{AGVs are not in operation} \end{cases} \quad (1)$$

In the formula, n is the number of AGVs in the transportation road network at time t , and $d_{(i,j)}^k(t)$ is the straight-line distance between the k -th AGV $N_{AGV}^{(k)}$ and point (i, j) at time t .

2.3 AGV State Transition Rules

Due to the situation of parking to avoid path conflict, the state of AGV is divided into two categories: parking and waiting and selecting the next path point.

The crowding degree threshold q is introduced to avoid collision between AGVs. When $\tau_{(j)j'} = 0$, it indicates that there is no AGV operation around the node (i', j') , and there is no danger of collision if this node is selected as the next path point. When $\tau_{(i',j')} = \lambda$, it indicates that the sum of the pheromone concentrations perceived by the node (i', j') is λ , which is equivalent to 1 AGV at this node. If this node is selected as the next path point, collision is very likely to occur. Therefore, this paper sets the range of the crowding degree threshold as $(0, \lambda)$. $allowed_k$ is the next set of path points for $N_{AGV}^{(k)}$. If $\tau_{(i',j')} (t) < q$, then taking (i', j') as the next waypoint, the possibility of collision is small, and it does not affect the normal operation of the transportation system, $(i', j') \in allowed_k$, $(i', j') \notin allowed_k$. If $allowed_k = 0$, then $N_{AGV}^{(k)}$ stops and waits. If $allowed_k = \emptyset$, then $N_{AGV}^{(k)}$ selects the next waypoint.

The selection of AGV path points is related to the attraction degree and heuristic function of the nodes to be selected. The attraction value of the node (i', j') to the AGV is represented by the difference between the crowdedness threshold q and the pheromone concentration $\tau_{(i',j')} (t)$ at the node (i', j') at time t , that is,

$$F_2^{(i',j')} = \frac{1}{d_{(i,j)}^{(i',j')}} \quad (3)$$

$$F_3^{(i',j')} = \frac{1}{d_{(i',j')}^{(e_x, e_y)}} \quad (4)$$

In the formula: $d_{(i,j)}^{(i',j')}$ is the straight-line distance between the node (i, j) and (i', j'); $d_{(i',j')}^{(e_x, e_y)}$ is the straight-line distance between (i', j') and the target point (e_x, e_y) .

The state transition probability of $N_{AGV}^{(k)}$ is:

$$P_{(i,j) \rightarrow (i',j')}^{(k)}(t) = \begin{cases} \frac{[F_1^{(i',j')}]^\alpha \cdot [F_2^{(i',j')}]^\beta \cdot [F_3^{(i',j')}]^\gamma}{\sum_{(i',j') \in allowed_k} [F_1^{(i',j')}]^\alpha \cdot [F_2^{(i',j')}]^\beta \cdot [F_3^{(i',j')}]^\gamma}, & (i', j') \in allowed_k \\ 0, & (i', j') \notin allowed_k \end{cases} \quad (5)$$

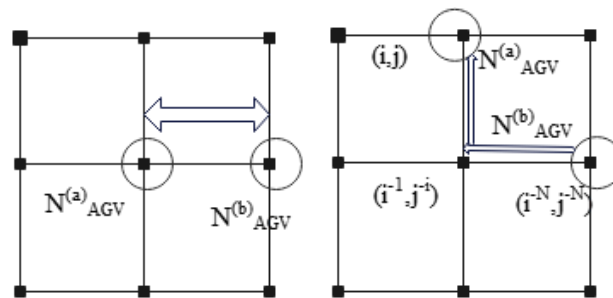
(6)

$$(i_0', j_0') = \arg \max_{(i',j')} P_{(i,j) \rightarrow (i',j')}^{(k)}$$

α, β, γ are the node attraction function $F_1^{(i',j')}$, the importance coefficients of the heuristic function $F_2^{(i',j')}$ and $F_3^{(i',j')}$, respectively. The next waypoint (i_0', j_0') is determined according to formula (6).

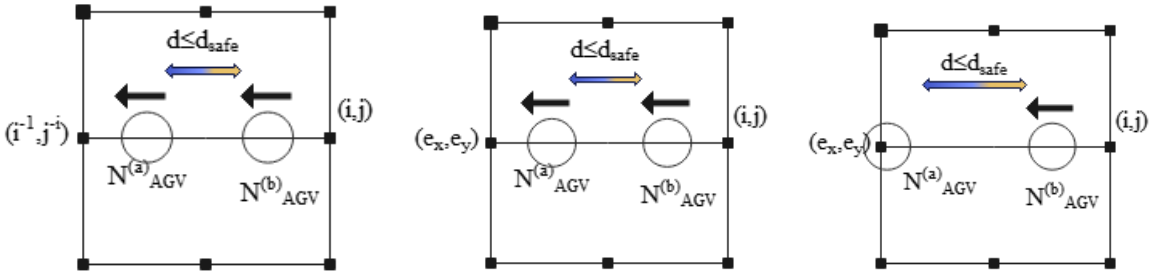
2.4 Conflict Detection and Resolution Mechanisms

According to the transportation characteristics of the automated terminal AGV, the conflict can be divided into two types: node conflict and path congestion, as shown in Figure 3 and Figure 4, respectively.



(a) Node conflict situation 1 (b) Node conflict situation 2

Figure 3: Schematic diagram of node conflict.



(a) Route congestion situation 1 (b) Route congestion situation 2 (c) Route congestion situation 3

Figure 4: Schematic diagram of path congestion.

This paper defines the conflict situations in various situations as follows:

Node conflict situation 1: Two AGVs are in adjacent nodes, and the paths to the next node overlap each other at the same time.

Node conflict situation 2: The two AGVs are not in adjacent nodes, but the next waypoint overlaps.

Path congestion situation 1: Two AGVs are located on the path between two nodes at the same time, in the same direction, and the distance is less than the safe distance.

Path congestion situation 2: Two AGVs are located on the path between the same node and the target point at the same time, the driving direction is the same, and the distance is less than the safety distance.

Path congestion situation 3: One AGV is at the target point for container loading and unloading operations, another AGV is heading to this target point, and the distance between the two AGVs is less than the safe distance.

The crowdedness threshold q can avoid node collision as shown in Figure 3(a).

We set:

$$S_{(i,j) \rightarrow (i',j')}^{(k)}(t) = \begin{cases} 1, N_{AGV}^{(k)} \text{ is on the path between } (i, j) \text{ and } (i', j') \text{ at time } t \\ 0, \text{ otherwise} \end{cases} \quad (7)$$

$$T_{(e_x, e_y)}^{(k)}(t) = \begin{cases} 1, N_{AGV}^{(k)} \text{ is loading or unloading in the target point } (e_x, e_y) \text{ at time } t \\ 0, \text{ otherwise} \end{cases} \quad (8)$$

$$S_{(i,j) \rightarrow (i',j')}^{(a)}(t) = S_{(i'',j'') \rightarrow (i',j')}^{(b)}(t) = 1 \quad (9)$$

$$\left| t_{(i',j')}^{(a)} - t_{(i',j')}^{(b)} \right| \leq \frac{d_{safe}}{v} \quad (10)$$

In the formula, $t_{(i',j')}^{(k)}$ is the moment when $N_{AGV}^{(k)}$ reaches the node (i', j') , d_{safe} is the safety distance between AGVs, and v is the driving speed of AGVs.

If formula (9) and formula (10) are satisfied at the same time, that is, at time t , $N_{AGV}^{(a)}$ and $N_{AGV}^{(b)}$ travel from (i, j) and (i'', j'') to (i', j') at the same time, respectively, and the time interval to reach node (i', j') is less than the time required to travel the safe distance, the CCS determines that the two AGVs have a node conflict as shown in Figure 4(b).

If the formulas (10) to (12), or the formulas (13) to (15), or the formulas (16) to (18) are satisfied at the same time, the CCS will determine that there is path congestion as shown in Figure 4(a), Figure 4(b) and Figure 4(c) respectively.

$$S_{(i,j) \rightarrow (i',j')}^{(a)}(t) = S_{(i'',j'') \rightarrow (i',j')}^{(b)}(t) = 1 \quad (11)$$

$$d_{(i_a, j_a)}^{(i', j')} \neq d_{(i_b, j_b)}^{(i', j')} \quad (12)$$

$$S_{(i,j) \rightarrow (e_x, e_y)}^{(a)}(t) = S_{(i'', j'') \rightarrow (e_x, e_y)}^{(b)}(t) = 1 \quad (13)$$

$$d_{(i_a, j_a)}^{(e_x, e_y)} \neq d_{(i_b, j_b)}^{(e_x, e_y)} \quad (14)$$

$$\left| t_{(e_x, e_y)}^{(a)} - t_{(e_x, e_y)}^{(b)} \right| \leq \frac{d_{safe}}{v} \quad (15)$$

$$T_{(e_x, e_y)}^{(a)}(t) = 1 \quad (16)$$

$$S_{(i,j) \rightarrow (e_x, e_y)}^{(b)}(t) = 1 \quad (17)$$

$$d_{(i_b, j_b)}^{(e_x, e_y)} \leq d_{safe} \quad (18)$$

In order to solve the problem of AGV path conflict in the horizontal transportation system of the automated terminal, for the node conflict, the comprehensive attraction value of the conflicting node to the two AGVs is compared to determine which AGV's next path point is the conflicting node. The

comprehensive attraction function of the conflict node (i', j') to $N_{AGV}^{(k)}$ is:

$$F_k^{(i', j')} = F_{1k}^{(i', j')} \cdot F_{2k}^{(i', j')} \cdot F_{3k}^{(i', j')} \quad (19)$$

In the formula, $F_{1k}^{(i', j')}$ is the attraction value of node (i', j') to $N_{AGV}^{(k)}$, $F_{2k}^{(i', j')}$ is the visibility between the current position of $N_{AGV}^{(k)}$ and node (i', j') . $F_{3k}^{(i', j')}$ is the visibility between node (i', j') and the target node $N_{AGV}^{(k)}$.

If $F_a^{(i,j)} > F_b^{(i,j)}$, then $N_{AGV}^{(a)}$ selects (i', j') as the next waypoint. If $F_a^{(i,j)} < F_b^{(i,j)}$, then $N_{AGV}^{(a)}$ selects (i', j') as the next waypoint. If $F_a^{(i,j)} = F_b^{(i,j)}$, a priority function will be established for judgment. The specific process is as follows. The map $f:A \rightarrow B$ as shown in Figure 5 is set.

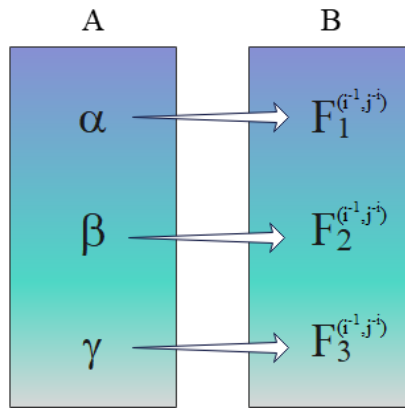


Figure 5: Schematic diagram of mapping.

The importance coefficients α , β , and γ corresponding to $F_1^{(i,j)}$, $F_2^{(i,j)}$, and $F_3^{(i,j)}$ form set A, and $F_1^{(i,j)}$, $F_2^{(i,j)}$, and $F_3^{(i,j)}$ form set B.

$$\mu = \max \{ \alpha, \beta, \gamma \} \quad (20)$$

$$\xi = \max \{ \{ \alpha, \beta, \gamma \} - \{ \mu \} \} \quad (21)$$

$$\varphi = \{ \alpha, \beta, \gamma \} - \{ \mu, \xi \} \quad (22)$$

$$P_1 = f(\mu) \quad (23)$$

$$P_2 = f(\xi) \quad (24)$$

$$P_3 = f(\varphi) \quad (25)$$

The maximum value μ , the intermediate value ξ and the minimum value φ of α , β and γ are sequentially determined by formula (20)-formula (22). The first priority function P_1 , the second

priority function P_2 and the third priority function P_3 are determined according to equations (23) to (25).

The first priority function P_{1k} of $N_{AGV}^{(k)}$ is first compared. If $P_{1a} < P_{1b}$, the conflict node (i', j') is the next path point of $N_{AGV}^{(b)}$. If $P_{1a} > P_{1b}$, the conflict node (i', j') is the next path point of $N_{AGV}^{(a)}$. If $P_{1a} = P_{1b}$, then the algorithm compares P_{2a} and P_{2b} , P_{3a} and P_{3b} step by step. If $P_{2a} = P_{2b}$ and $P_{3a} = P_{3b}$, the CCS randomly decides which AGV chooses (i', j') as the next waypoint. Another AGV selects other nodes in its allowed, and if there are no other nodes in allowed, it stops and waits. In response to path congestion, the CCS controls the distance between the two AGVs to a safe distance d_{safe} and then stops. In order to ensure transportation safety, the CCS needs to determine the total number and types of conflicts in the horizontal transportation area in real time, and use the above methods to resolve the conflicts. Therefore, this part designs an AGV path conflict resolution mechanism for the CCS pair. The specific process is shown in Figure 6.

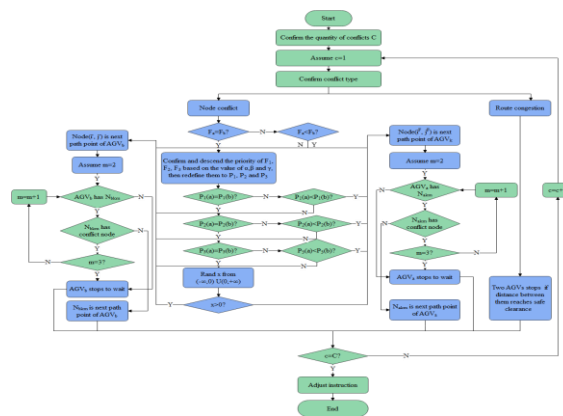


Figure 6: Flowchart of the conflict resolution mechanism.

The specific steps of the conflict resolution mechanism are as follows:

S1: The CCS determines the total number C of AGV vehicles in conflict, and sets the intermediate variable $c=1$.

S2: The system determines the conflict type of the c -th car in conflict. If it is a node conflict, the system goes to S3. If the path is congested, the system controls the two AGVs to stop at a safe distance after the distance, and enter S22.

S3: The system determines the optional next path point sets AGV_a and AGV_b corresponding to $allowed_a$ and $allowed_b$ according to the crowding degree threshold q , and sorts the nodes according to the state transition probability of each node in $allowed_a$ and $allowed_b$ in descending order. The state transition probability is the state transition probability from the node where the AGV

vehicle is currently located to the node in the set, and N_{km} represents the node in the selection sequence m in the optional next waypoint set $allowed_k$ corresponding to the kth AGV vehicle AGV_k .

S4: According to the calculation formula of the comprehensive attraction value $F_k^{(i',j')}$ of the k-th AGV vehicle AGV_k by the conflict node (i', j'), the system calculates the comprehensive attraction value $F_a^{(i',j')}$ and $F_b^{(i',j')}$ of the two AGV vehicles AGV_a and AGV_b in conflict, and judges whether it satisfies $F_a^{(i',j')} = F_b^{(i',j')}$. If it is satisfied, the system goes to S6, otherwise, goes to S5.

S5: The system judges whether $F_a^{(i',j')} < F_b^{(i',j')}$ is satisfied. If it is satisfied, the system goes to S15, otherwise, goes to S14.

S6: According to the weight coefficients α, β, γ of $F_{1k}^{(i',j')}$, $F_{2k}^{(i',j')}$ and $F_{3k}^{(i',j')}$ set, the priorities of $F_{1k}^{(i',j')}$, $F_{2k}^{(i',j')}$ and $F_{3k}^{(i',j')}$ are determined from large to small, and the values of P_{1k} , P_{2k} and P_{3k} are determined, wherein the subscript k represents the serial number.

S7: The system judges whether $P_{1a} = P_{1b}$ is satisfied. If it is satisfied, the system goes to S9, otherwise, goes to S8.

S8: The system judges whether $P_{1a} < P_{1b}$ is satisfied. If it is satisfied, the system goes to S15, otherwise, goes to S14.

S9: The system judges whether $P_{2a} = P_{2b}$ is satisfied. If it is satisfied, the system goes to S11, otherwise, goes to S10.

S10: The system judges whether $P_{2a} < P_{2b}$ is satisfied. If it is satisfied, the system goes to S15, otherwise, goes to S14.

S11: The system judges whether $P_{3a} = P_{3b}$ is satisfied. If it is satisfied, the system goes to S13, otherwise, goes to S12.

S12: The system judges whether $P_{3a} < P_{3b}$ is satisfied. If it is satisfied, the system goes to S15, otherwise, goes to S14.

S13: The algorithm selects any real number from the interval $(-\infty, 0) \cup (0, +\infty)$ and determines whether it is greater than 0. If it is greater than 0, the algorithm goes to S14, otherwise, goes to S15.

S14: The system sets the node (i', j') as the next path point of the a-th AGV vehicle AGV_a . At this time, the next path point of the b-th AGV vehicle AGV_b needs to be determined, so the system sets k=b and goes to S16.

S15: The system sets the node (i', j') as the next path point of the b -th AGV vehicle AGV_b . At this time, the next path point of the a -th AGV vehicle AGV_a needs to be determined, so the system sets $k=b$ and goes to S16.

S16: The system sets $m=2$.

S17: The system determines whether there is a node N_{km} with a selection order of m in the next optional path point set $allowed_k$ corresponding to the k -th AGV vehicle AGV_k . If it exists, the system goes to S18, otherwise, goes to S20.

S18: The system judges whether there is a node conflict on node N_{km} . If there is a node conflict, the system goes to S19, otherwise, goes to S21.

S19: The system judges whether $m=3$ is established. If it is established, the system goes to S20. If it is not established, $m=m+1$ on the system, and return to S17.

S20: The k -th AGV vehicle AGV_k stops and waits, and the system enters S22.

S21: N_{km} is the next path point of the k th AGV vehicle AGV_k , and the system enters S22.

S22: The system judges whether $c=C$ is established. If it is established, the system ends, otherwise, the system sets $c=c+1$ and returns to S2.

3 VERIFICATION OF SYSTEM PERFORMANCE

In this paper, taking AGV vehicle as an example, the path optimization algorithm is applied to the control of AGV. First of all, this paper evaluates the electrical control effect and stability with the simulation test, and the results shown in Figure 7 and Figure 8 are obtained.

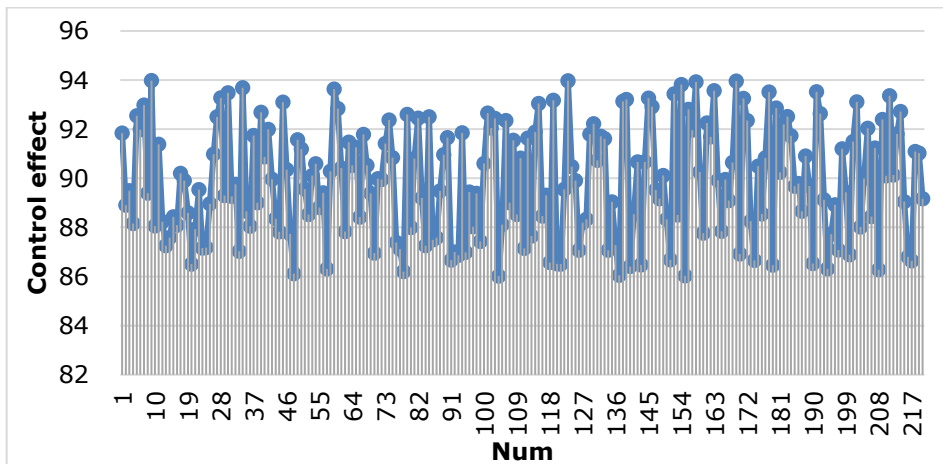


Figure 7: Evaluation of the control effect of the EACS based on the path optimization hybrid algorithm.

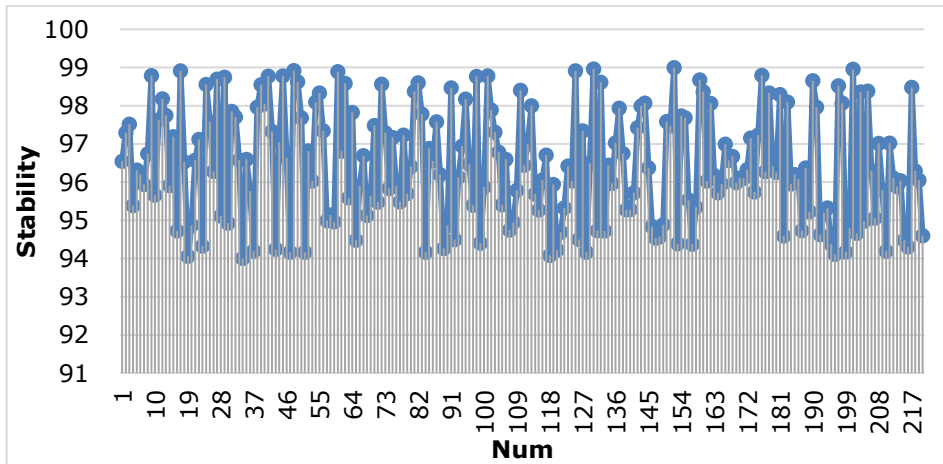


Figure 8: Evaluation of control stability of EACS based on path optimization hybrid algorithm.

It can be seen from the above research that the control effect and control stability of the EACS based on the path optimization hybrid algorithm in this problem are good, which is helpful to the control improvement of the EACS.

4 CONCLUSION

As an important part of the power and electrical system, the electric power ACS is closely connected with the platform control system, and can accept the signals from the CCS or the site, and execute actions according to the relevant instructions to play its own functions. Most of the industry uses DCS control system to control each electrical control point point-to-point. Each electrical control point is organically linked to the system and then connected to an analog-to-digital converter. Then, the incoming signal is converted into a digital signal and presented on the operation interface for the operator to operate in combination with the on-site situation and actual needs. From the perspective of function, it can be known that the electric power ACS is mainly divided into three parts: the electrical control center, the driving device, and the electrical transformation. In this paper, the EACS is designed by combining the path optimization algorithm, and an EACS is proposed. Moreover, combined with the path optimization hybrid algorithm, this paper takes the control of the AGV vehicle as a case to study the algorithm effect. The research shows that the control effect and control stability of the EACS based on the path optimization hybrid algorithm are good.

Pengxiao Ji, <https://orcid.org/0000-0002-7819-7881>

REFERENCES

- [1] Gehrmann, C.; Gunnarsson, M.: A digital twin based industrial automation and control system security architecture, *IEEE Transactions on Industrial Informatics*, 16(1), 2019, 669-680. <https://doi.org/10.1109/TII.2019.2938885>
- [2] Jansi, M. S.; Elaiyarani, M. K.: IOT based home automation system, *Turkish Journal of Computer and Mathematics Education (TURCOMAT)*, 11(3), 2020, 2246-2253.

- [3] Kryukov, O. V.; Gulyaev, I. V.; Teplukhov, D. Y.: Method for stabilizing the operation of synchronous machines using a virtual load sensor, *Russian Electrical Engineering*, 90(7), 2019, 473-478. <https://doi.org/10.3103/S1068371219070083>
- [4] Liang, W.; Zheng, M.; Zhang, J.; Shi, H.; Yu, H.; Yang, Y.; Zhao, X.: WIA-FA and its applications to digital factory: A wireless network solution for factory automation, *Proceedings of the IEEE*, 107(6), 2019, 1053-1073. <https://doi.org/10.1109/JPROC.2019.2897627>
- [5] Pratap, B.; Purwar, S.: Real-time implementation of nonlinear state and disturbance observer-based controller for twin rotor control system, *International Journal of Automation and Control*, 13(4), 2019, 469-497. <https://doi.org/10.1504/IJAAC.2019.100471>
- [6] Rahim, M. K. A. A.; Zahari, M. H.; Rahimi, M. F. F.; Amin, Z. M.: Home Automation Controller with Security System. *Multidisciplinary Applied Research and Innovation*, 3(1), 2022, 475-481.
- [7] Saraswat, M.; Sharma, K.; Chauhan, N. R.; Shukla, R. K.: Role of automation in energy management and distribution, *Journal of Scientific and Industrial Research (JSIR)*, 79(10), 2020, 951-954. <https://doi.org/10.56042/jsir.v79i10.43593>
- [8] Shen, Q.; Yue, C.; Goh, C. H.; Wang, D.: Active fault-tolerant control system design for spacecraft attitude maneuvers with actuator saturation and faults, *IEEE Transactions on Industrial Electronics*, 66(5), 2018, 3763-3772. <https://doi.org/10.1109/TIE.2018.2854602>
- [9] Skouras, T. A.; Gkonis, P. K.; Ilias, C. N.; Trakadas, P. T.; Tsampasis, E. G.; Zahariadis, T. V.: Electrical vehicles: Current state of the art, future challenges, and perspectives, *Clean Technologies*, 2(1), 2019, 1-16. <https://doi.org/10.3390/cleantechnol2010001>
- [10] Wang, K.; Tian, E.; Liu, J.; Wei, L.; Yue, D.: Resilient control of networked control systems under deception attacks: a memory-event-triggered communication scheme, *International Journal of Robust and Nonlinear Control*, 30(4), 2020, 1534-1548. <https://doi.org/10.1002/rnc.4837>
- [11] Wei, C.; Benosman, M.; Kim, T.: Online parameter identification for state of power prediction of lithium-ion batteries in electric vehicles using extremum seeking, *International Journal of Control, Automation and Systems*, 17(11), 2019, 2906-2916. <https://doi.org/10.1007/s12555-018-0506-y>
- [12] Xiang, B.; Liu, X.; Chen, Y.: Event-based Networked Predictive Control Systems with Secure Transmission Protocol, *International Journal of Control, Automation and Systems*, 20(4), 2022, 1076-1086. <https://doi.org/10.1007/s12555-021-0265-z>
- [13] Xu, D.; Wang, B.; Zhang, G.; Wang, G.; Yu, Y.: A review of sensorless control methods for AC motor drives, *CES Transactions on Electrical Machines and Systems*, 2(1), 2018, 104-115. <https://doi.org/10.23919/TEMS.2018.8326456>
- [14] Yang, C.; Peng, G.; Cheng, L.; Na, J.; Li, Z.: Force sensorless admittance control for teleoperation of uncertain robot manipulator using neural networks, *IEEE Transactions on Systems, Man, and Cybernetics: Systems*, 51(5), 2019, 3282-3292. <https://doi.org/10.1109/TSMC.2019.2920870>
- [15] Yuan, Y.; Yuan, H.; Ho, D. W.; Guo, L.: Resilient control of wireless networked control system under denial-of-service attacks: A cross-layer design approach, *IEEE Transactions on Cybernetics*, 50(1), 2018, 48-60. <https://doi.org/10.1109/TCYB.2018.2863689>
- [16] Zhang, M.; Zhang, Y.; Cheng, X.: An enhanced coupling PD with sliding mode control method for underactuated double-pendulum overhead crane systems, *International Journal of Control, Automation and Systems*, 17(6), 2019, 1579-1588. <https://doi.org/10.1007/s12555-018-0646-0>
- [17] Zinchenko, S.; Mateichuk, V.; Nosov, P.; Popovych, I.; Solovey, O.; Mamenko, P.; Grosheva, O.: Use of simulator equipment for the development and testing of vessel control systems, *The Scientific Journal of Riga Technical University-Electrical, Control and Communication*

- Engineering, 16(2), 2020, 58-64. <https://doi.org/10.2478/ecce-2020-0009>
- [18] Zuo, Y.; Zhu, X.; Quan, L.; Zhang, C.; Du, Y.; Xiang, Z.: Active disturbance rejection controller for speed control of electrical drives using phase-locking loop observer, IEEE Transactions on Industrial Electronics, 66(3), 2018, 1748-1759. <https://doi.org/10.1109/TIE.2018.2838067>